did not change by more than 1.5% throughout these studies, for either source. The distances through the column obtained prior to the experiments with FT–300 wax in the large column are given in Table 3.8. The distances are similar to the left and right of the center of the column for each source. The differences in the distance through the column for the two sources may be due to slightly different radial locations and/or axial locations.

Gas Holdups in Two – Phase Systems

Experiments were conducted using both two–phase (gas/liquid) and three–phase (gas/liquid/solid) systems. For two–phase experiments, gas holdups were obtained using each density gauge and the values compared. As described above, measurements were made at various radial and axial locations. The gas holdup at a given radial position, for both sources was calculated using:

$$\epsilon_{r_i} = 1 - \frac{\ln(B_i / B_{o_i})}{-d_i \mu_\ell} \tag{3.37}$$

Axial gas holdups were obtained from a volumetric weighted average of the radial gas holdups at a given axial location. Knowing the distance through the column at each radial position, d_i, and the column diameter, d_c, the radial position (measured from the center), r_{pos_i}, is

$$r_{pos_i} = \frac{\sqrt{d_c^2 - d_i^2}}{2} \tag{3.38}$$

Since the distances through the column did not vary significantly with axial position or column side (i.e. left or right of center), average values for r_{pos_i} and d_i were used to obtain the volumetric weights, w_i, needed to calculate the gas holdup at each axial location (see Eq. 3.40). The average values for r_{pos_i} and d_i that were used to calculate the weights are shown in Figure 3.14.

Table 3.8. Distance Through the Column for Both Sources at All Locations for the Experiments with FT–300 Wax

HEIGHT (m)	SOURCE	DISTANCE THROUGH THE COLUMN[a], d_i (m) 1	2	3	4	5	6
0.9	Co–60	16.10	18.62	20.23	20.11	18.42	16.30
	Cs–137	16.31	18.69	19.87	19.90	18.51	16.41
1.5	Co–60	15.81	18.77	20.07	20.06	18.76	16.49
	Cs–137	15.79	18.17	19.85	20.26	18.83	16.96
2.1	Co–60	16.33	18.97	20.31	20.45	18.87	16.63
	Cs–137	15.60	18.64	19.91	20.04	18.74	16.59

[a] Radial positions corresponding to numbers (1 to 6) are shown in Figures 3.13 and 3.14

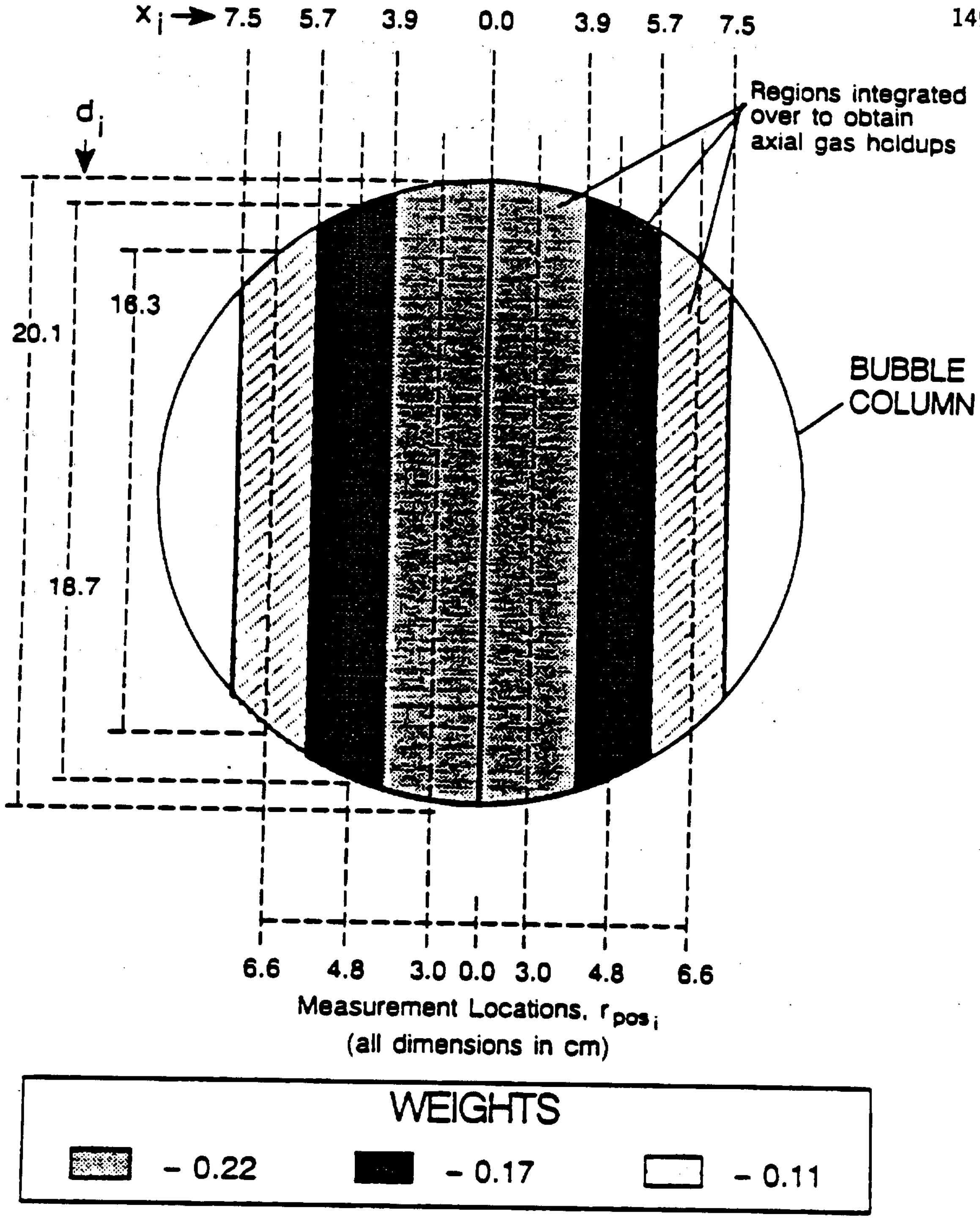

Figure 3.14. Schematic representation of the locations for radial measurements with the nuclear density gauge apparatus.

The column was divided into six sections (shaded regions in Figure 3.14) surrou ing each measurement location. The cross-sectional area in a given shaded region, divided by the total area of the shaded regions was used as the weighting factor for measurements made in that region. The area of region i, A_{s_i} is given by:

$$A_{s_i} = [x_{i+1}\sqrt{r_c^2 - x_{i+1}^2} + r_c^2 \sin^{-1}(x_{i+1} / r_c)] - [x_i\sqrt{r_c^2 - x_i^2} + r_c^2 \sin^{-1}(x_i / r_c)] \quad (3.39)$$

where r_c is the radius of the column and x_i and x_{i+1} are the distances (measured from the center of the column) bounding the region to be evaluated. In particular, the values of x_i and x_{i+1} that were used are (0,3.9), (3.9,5.7), and (5.7,7.5). The area of each section was divided by the total area integrated over (i.e. sum of the area of each section) to obtain the appropriate weighting factor, w_i

$$w_i = \frac{A_{s_i}}{\sum_{i=1}^{6} A_{s_i}} \quad (3.40)$$

The weights obtained are given in Figure 3.14. The gas holdup at a given axial position was then calculated from:

$$\epsilon_{gax} = \sum_i \epsilon_{r_i} w_i \qquad i = 1 \text{ to } 6 \quad (3.41)$$

where ϵ_{gax} is the axial gas holdup and ϵ_{r_i} (see Eq. 3.37) is the radial gas holdup at location i.

Once axial gas holdups have been calculated, average gas holdups may be calculated. Recall that the average gas holdup is defined as

$$\epsilon_g = \frac{\text{volume of gas in the dispersion}}{\text{volume of the dispersion}} \quad (3.42)$$

Assuming the column can be divided into i sections, Eq. 3.42 may be rewritten as

$$\epsilon_g = \sum_i \frac{V_{g_i}}{V_{sect_i}} \frac{V_{sect_i}}{V_{exp}} = \sum_i \epsilon_{gax_i} \frac{h_i}{h_{exp}} \quad (3.43)$$

where V_{g_i} is the volume of gas in section i, V_{sect_i} is the total volume of section i, V_{exp} is the total volume of the dispersion, ϵ_{gax_i} is the gas holdup in section i, h_i is the length of section i, and h_{exp} is the expanded height of the slurry. Assuming h_i approaches 0, Eq. 3.43 may be rewritten in integral form as

$$\epsilon_g = \frac{1}{h_{exp}} \int_0^{h_{exp}} \epsilon_{gax} dh \qquad (3.44)$$

Since measurements were made at three axial locations only, one may estimate the average gas holdup using various techniques. Three different approaches were examined in this study. First, the axial gas holdup data may be fitted to a curve. The equation for the curve may then be substituted into Eq. 3.44 for ϵ_{gax_i} to obtain an estimate for the average gas holdup. The second approach, uses the discretized form of Eq. 3.44 (i.e. Eq. 3.43) to obtain an estimate for the average gas holdup. Since measurements are made at three locations, the column may be divided into three sections. The sections used were (1) 0 to 1.2 m above the distributor, (2) 1.2 to 1.8 m above the distributor, and (3) 1.8 m above the distributor to the top of the dispersion (maximum of 3 m for continuous slurry flow). Thus, the values of h_i are 1.2 m, 0.6 m, and <1.2 m. (see Figure 3.15). The third, and simplest approach would be to weight each axial gas holdup evenly. Using this approach, the average gas holdup is

$$\epsilon_g = \sum_i \frac{\epsilon_{gax_i}}{n} \qquad i = 1 \text{ to } 3 \qquad (3.45)$$

Since axial gas holdups did not vary significantly, there were no significant differences in the values of gas holdup estimated using the three different approaches. Table 3.9 compares average gas holdups obtained using the three techniques described above for data obtained at gas velocities of 0.02 and 0.09 m/s, during experiment number 4 in Table 2.5. This experiment was conducted in the continuous mode of operation. As shown in Table 3.9a there is very little difference in gas holdups obtained using

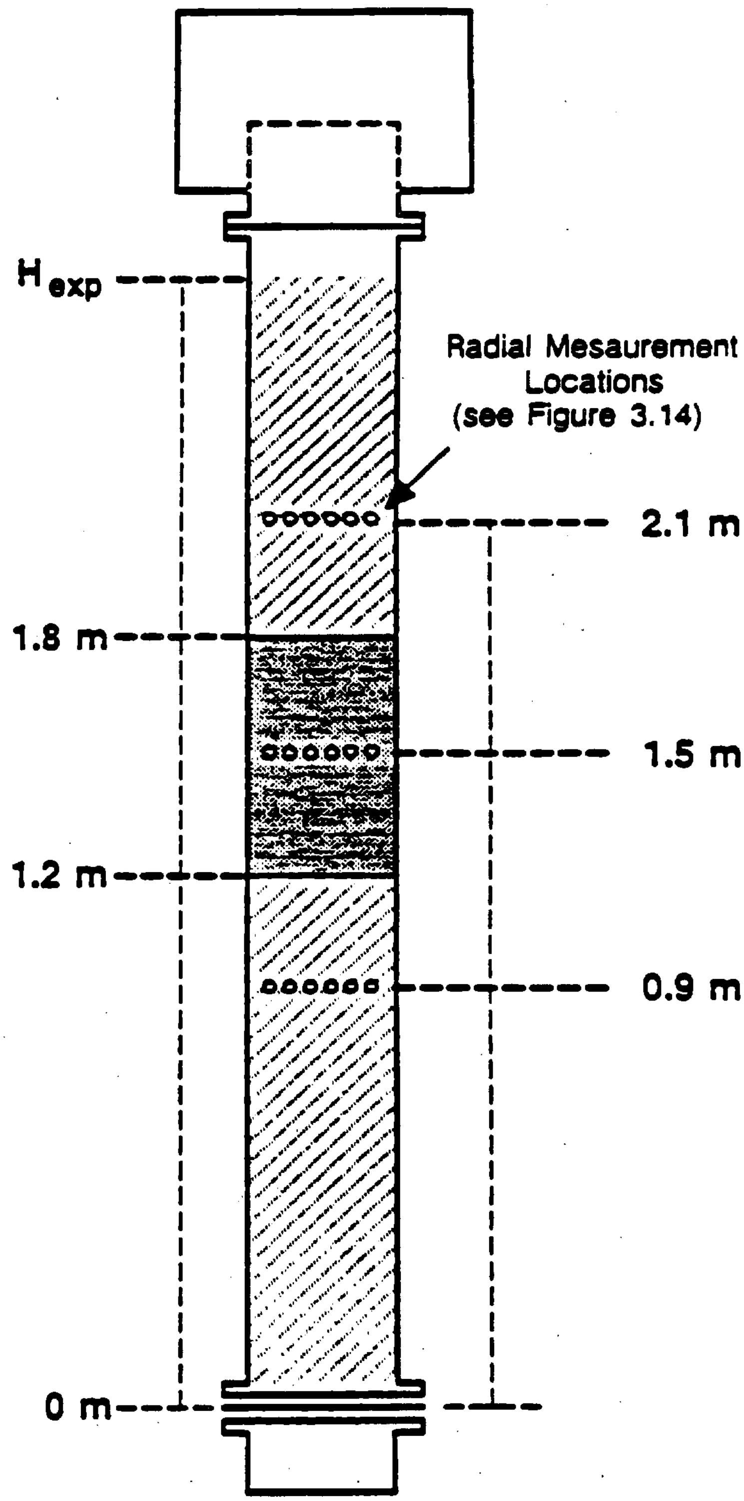

Figure 3.15. Schematic diagram of the regions used to obtain average gas holdups.

Table 3.9a. Effect of Technique Used to Obtain Average Gas Holdups from Axial Gas Holdups (Data from Experiment 4 in Table 2.5, $u_g = 0.02$ m/s)

EXP. HEIGHT (m)	HEIGHT (m)			ϵ_g^a	ϵ_g^b	ϵ_g^c
	0.9	1.5	2.1			
2.6[d]	0.0947	0.1083	0.1323	0.106	0.109	0.112
3.0[e]	0.0947	0.1083	0.1323	0.114	0.116	0.112

[a] Obtained from Eq. 3.44
[b] Obtained from Eq. 3.43
[c] Obtained from Eq. 3.45
[d] Representative of a batch mode experiment
[e] Representative of a continuous mode experiment, column height is 3.0 m

Table 3.9b. Effect of Technique Used to Obtain Average Gas Holdups from Axial Gas Holdups (Data from Experiment 4 in Table 2.5, $u_g = 0.09$ m/s)

EXP. HEIGHT (m)	HEIGHT (m)			ϵ_g^a	ϵ_g^b	ϵ_g^c
	0.9	1.5	2.1			
2.6[d]	0.2342	0.2446	0.2637	0.245	0.246	0.247
3.0[e]	0.2342	0.2446	0.2637	0.252	0.249	0.247

[a] Obtained from Eq. 3.44
[b] Obtained from Eq. 3.43
[c] Obtained from Eq. 3.45
[d] Representative of a batch mode experiment
[e] Representative of a continuous mode experiment, column height is 3.0 m

the various approaches. The data from this experiment were also analyzed assumi⁻⁻ an expanded height of only 2.6 m (i.e. simulate a batch experiment). For this case (see Table 3.9b), the differences in the calculated gas holdups were slightly greater than those for the continuous case; however, they were still relatively small ($< 6\%$ difference). Thus, for simplicity, Eq. 3.45 was used to estimate the average gas holdup for all experiments.

Gas Holdups in Three – Phase Systems

Gas holdups for three–phase systems were calculated by treating all three phases independently, as well as, by treating the three–phase system as a two–phase system (i.e. grouping the liquid and solid phases together). When treating the three–phase system as a two–phase system, Eq. 3.37 is used to calculate radial gas holdups by replacing the liquid phase attenuation coefficient, μ_ℓ with the slurry phase attenuation coefficient, $\mu_{s\ell}$ (see Eq.3.30). If all three phases are treated separately, then Eqs. 3.16, 3.17, and 3.18 may be used to calculate radial gas holdups. Once radial gas holdı are obtained, axial and average gas holdups are calculated using Eqs. 3.41 and 3.45, respectively.

Discussion of Results

Radial, axial and average gas holdups were measured with the nuclear density gauge during two–phase and three–phase experiments in the 0.21 m ID column. Data collected during all experiments were analyzed assuming Case I alignment. Furthermore, data from three–phase experiments were analyzed by two different methods: (1) treat all three phases independently and (2) group liquid and solids together to form a pseudo two–phase system.

Independent Treatment of all Three – Phases

Gas holdup values obtained from nuclear density gauge measurements, treating all three phases independently, were not good. However, this was not surprising, since sensitivity analysis revealed that very small errors in the count rate could produce substantial errors in volume fractions for the Co–60/Cs–137 system (see Table 3.3).

Data acquired from the density gauges during several experiments were analyzed to obtain radial gas holdups. Table 3.10a shows radial gas holdup values obtained from the batch experiment with 20 wt%, 20 – 44μm iron oxide particles in FT–300 wax. Radial gas holdups varied significantly for each gas velocity. In order to see what effect slight errors in the path length through the column, d, had on the gas holdups, it was varied. These results are shown in Table 3.10b for the experiment with FT–300 wax. We assumed that the volume fraction of solids did not vary with radial position and adjusted the value of d, until the volume fraction of solids, ϵ_s, was similar to that obtained from analysis of the slurry sample withdrawn at the same height of the density gauge measurement (see Figure 3.13). Once similar values of ϵ_s were obtained, axial gas holdups were calculated from the radial gas holdups using Eq. 3.41, and these values were compared to those values obtained at the same location (for this case, the axial gas holdups were compared to the measured gas holdups between pressure transducers 3 and 4; see Figure 3.13) using conventional techniques (see Chapter II). As shown in Table 3.10b, there was excellent agreement between axial gas holdups obtained using the different techniques. Also shown in Tables 3.10a and 3.10b is the distance through the column, d, for the high and low energy source, before and after altering its value, respectively. A range of values is presented in Table 3.10b, since different values of d were used at each gas velocity. For all experiments, the maximum percent difference between the measured value of d for each source and the altered value of d for each source at each radial location was less than 4%, and usually less than 2%. Thus

Table 3.10a. Gas holdups from Measurements with the Nuclear Density Gauge at a Height of 1.5 m Above the Distributor (FT-300 Wax, 20 wt% 20 – 44 μm Iron Oxide)

u_g	Radial Position[a]					
(m/s)	6.6	4.8	3.0	3.0	4.8	6.6
0.02	0.06	0.24	0.04	0.21	0.37	0.24
0.04	-0.09	0.27	0.03	0.23	0.07	0.16
0.08	-0.03	0.19	0.12	0.31	0.45	0.14
0.12	0.13	0.18	0.12	0.35	0.48	0.13
d_L^b	16.96	18.17	20.26	19.85	18.83	15.79
d_H^c	16.49	18.76	20.06	20.07	18.77	15.81

[a] – Measured from the center of the column (cm)
[b] – Distance through the column for the Cs–137 source (cm)
[c] – Distance through the column for the Co–60 source (cm)

Table 3.10b. Gas and Solids Holdups from Measurements with the Nuclear Density Gauge at a Height of 1.5 m Above the Distributor After Modifying the Thickness (d) of the Absorbing Media (FT-300 Wax, 20 wt% 20 – 44 μm Iron Oxide)

u_g	RADIAL POSITION[a]						ϵ_g^b	ϵ_g^c	ϵ_s^b	ϵ_s^c
(m/s)	6.6	4.8	3.0	3.0	4.8	6.6				
0.02	0.117	0.124	0.128	0.129	0.124	0.105	0.122	0.128	0.015	0.016
0.04	0.159	0.164	0.194	0.183	0.166	0.150	0.172	0.189	0.024	0.024
0.08	0.161	0.210	0.213	0.221	0.198	0.194	0.202	0.172	0.026	0.024
0.12	0.189	0.197	0.223	0.222	0.215	0.185	0.210	0.216	0.021	0.025
d_L^d	16.86-16.98	18.15-18.19	20.10-20.28	19.75-19.95	18.79-18.87	15.69-15.79				
d_H^e	16.6-16.8	18.9	20.25	19.9	18.8	15.6-15.9				

[a] – Measured from the center of the column (cm)
[b] – Axial holdups from nuclear density gauge measurements
[c] – Axial holdups from conventional measurements (Chapter II)
[d] – Range of values for the distance through the column for the Cs–137 source (cm)
[e] – Range of values for the distance through the column for the Co–60 source (cm)

indicating once again, that slight errors in the measured quantities (i.e. count rate, distance through the column, etc.) have a significant effect on the calculated holdups, when two "high" energy sources are employed. Data obtained from other experiments were also analyzed treating all three–phases independently. The results from these experiments are shown in Tables 3.11 to 3.14. Tables 3.11a and 3.11b show results obtained from the batch mode experiment with 20 wt% large silica particles in SASOL wax at a height of 1.5 m above the distributor. Results from this experiment were similar to those obtained during the experiment with large iron oxide particles suspended in FT–300 wax (Table 3.10). Namely, there was a significant variation in radial gas holdup profiles when the measured distances were used; however, upon slightly adjusting the distance through the column, more uniform radial holdup values were obtained. Axial holdups calculated from the modified radial profiles were comparable to those using conventional techniques (see Chapter II) were obtained. Similar results were also obtained at different heights and with small iron oxide particles. Radial gas holdup profiles for the experiment conducted with 20 – 44 μm iron oxide particles in FT–300 wax at a height of 2.1 m above the distributor are shown in Table 3.12. Results from the experiment with large silica particles in SASOL wax, at a height of 0.9 m above the distributor are shown in Table 3.13, and results from the experiment with small iron oxide particles at a slurry velocity of 0.005 m/s at a height of 1.5 m above the distributor are shown in Table 3.14.

Two – Phase and Pseudo Two – Phase Results

Figures 3.16 to 3.19 show radial gas holdup profiles at a height of 1.5 m above the distributor obtained from different experiments in two–phase (Figure 3.16) and three–phase systems (Figures 3.17, 3.18, and 3.19). The results shown for the three–phase system were obtained by treating it as a pseudo two–phase system (i.e. the liquid and solid phases were grouped together). Radial gas holdups for three–phase experiments

Table 3.11a. Gas Holdups from Measurements with the Nuclear Density at a Height of 1.5 m Above the Distributor (SASOL Wax, 20 wt% 20 – 44 μm Silica)

u_g	Radial Position[a]			
(m/s)	6.6	3.0	3.0	6.6
0.02	0.34	0.12	0.15	0.21
0.04	0.23	0.17	0.16	0.24
0.08	0.32	0.30	0.26	0.42
0.12	0.30	0.33	0.34	0.46
d_L^b	16.65	20.44	20.49	15.99
d_H^c	16.55	20.31	20.41	15.9

[a] – Measured from the center of the column (cm)
[b] – Distance through the column for the Cs–137 source (cm)
[c] – Distance through the column for the Co–60 source (cm)

Table 3.11b. Gas and Solids Holdups from Measurements with the Nuclear Density Gauge at a Height of 1.5 m Above the Distributor After Modifying the Thickness (d) of the Absorbing Media (SASOL Wax, 20 wt% 20 – 44 μm Silica)

u_g	RADIAL POSITION[a]				ϵ_g^b	ϵ_g^c	ϵ_s^b	ϵ_s^c
(m/s)	6.6	3.0	3.0	6.6				
0.02	0.104	0.116	0.120	0.115	0.117	0.115	0.067	0.066
0.04	0.146	0.168	0.162	0.143	0.157	0.150	0.066	0.066
0.08	0.206	0.224	0.230	0.207	0.218	0.191	0.070	0.065
0.12	0.205	0.262	0.266	0.225	0.244	0.253	0.067	0.066
d_L^d	16.5-16.95	20.45-20.49	20.49-20.59	16.3-16.4				
d_H^e	16.2	20.3	20.4	15.9				

[a] – Measured from the center of the column (cm)
[b] – Axial holdups from nuclear density gauge measurements
[c] – Axial holdups from conventional measurements (Chapter II)
[d] – Range of values for the distance through the column for the Cs–137 source (cm)
[e] – Range of values for the distance through the column for the Co–60 source (cm)

Table 3.12a. Gas Holdups from Measurements with the Nuclear Density Gauge at a Height of 2.1 m Above the Distributor (FT-300 Wax, 20 wt% 20 – 44 μm Iron Oxide)

u_g (m/s)	Radial Position[a] 6.6	4.8	3.0	3.0	4.8	6.6
0.02	0.03	0.02	0.07	0.13	0.08	-0.04
0.04	0.30	0.39	0.34	0.61	0.41	0.36
0.08	0.04	0.06	0.08	0.47	0.11	-0.01
0.12	0.02	-0.02	0.06	0.27	0.18	0.12
d_L^b	16.60	18.64	19.91	20.04	18.91	16.59
d_H^c	16.33	18.97	20.31	20.45	18.87	16.63

[a] – Measured from the center of the column (cm)
[b] – Distance through the column for the Cs–137 source (cm)
[c] – Distance through the column for the Co–60 source (cm)

Table 3.12b. Gas and Solids Holdups from Measurements with the Nuclear Density Gauge at a Height of 2.1 m Above the Distributor After Modifying the Thickness (d) of the Absorbing Media (FT-300 Wax, 20 wt% 20 – 44 μm Iron Oxide)

u_g (m/s)	RADIAL POSITION[a] 6.6	4.8	3.0	3.0	4.8	6.6	ϵ_g^b	ϵ_g^c	ϵ_s^b	ϵ_s^c
0.02	0.131	0.152	0.171	0.169	0.149	0.140	0.151	0.137	0.014	0.014
0.04	0.220	0.279	0.282	0.301	0.280	0.259	0.271	0.274	0.023	0.021
0.08	0.161	0.230	0.233	0.260	0.211	0.187	0.221	0.232	0.023	0.023
0.12	0.170	0.247	0.261	0.272	0.251	0.219	0.224	0.240	0.023	0.024
d_L^d	16.4-16.5	18.1-18.4	19.5-20.0	20.0-20.5	18.6-19.0	16.1-16.4				
d_H^e	16.33	18.97	20.31	20.45	18.87	16.63				

[a] – Measured from the center of the column (cm)
[b] – Axial holdups from nuclear density gauge measurements
[c] – Axial holdups from conventional measurements (Chapter II)
[d] – Range of values for the distance through the column for the Cs–137 source (cm)
[e] – Range of values for the distance through the column for the Co–60 source (cm)

Table 3.13a. Gas Holdups from Measurements with the Nuclear Density Gauge at a Height of 0.9 m Above the Distributor (SASOL Wax, 20 wt% 20 – 44 μm Silica)

u_g	Radial Position[a]			
(m/s)	6.6	3.0	3.0	6.6
0.02	0.11	0.10	0.18	0.01
0.04	0.19	0.11	0.14	0.11
0.08	0.36	0.29	0.25	0.29
0.12	0.22	0.25	0.21	0.32
d_L^b	16.32	19.84	19.92	16.39
d_H^c	16.41	20.19	20.09	16.52

[a] – Measured from the center of the column (cm)
[b] – Distance through the column for the Cs–137 source (cm)
[c] – Distance through the column for the Co–60 source (cm)

Table 3.13b. Gas and Solids Holdups from Measurements with the Nuclear Density Gauge at a Height of 0.9 m Above the Distributor After Modifying the Thickness (d) of the Absorbing Media (SASOL Wax, 20 wt% 20 – 44 μm Silica

u_g	RADIAL POSITION[a]				ϵ_g^b	ϵ_g^c	ϵ_s^b	ϵ_s^c
(m/s)	6.6	3.0	3.0	6.6				
0.02	0.08	0.11	0.12	0.08	0.10	0.10	0.08	0.07
0.04	0.10	0.13	0.13	0.09	0.12	0.14	0.07	0.07
0.08	0.17	0.20	0.20	0.16	0.18	0.14	0.07	0.07
0.12	0.18	0.22	0.21	0.18	0.20	0.20	0.07	0.06
d_L^d	16.4-16.9	19.8-20.2	19.95-20.1	16.2-16.6				
d_H^e	16.4	20.2	20.1	16.5				

[a] – Measured from the center of the column (cm)
[b] – Axial holdups from nuclear density gauge measurements
[c] – Axial holdups from conventional measurements (Chapter II)
[d] – Range of values for the distance through the column for the Cs–137 source (cm)
[e] – Range of values for the distance through the column for the Co–60 source (cm)

Table 3.14a. Gas Holdups from Measurements with the Nuclear Density Gauge at a Height of 1.5 m Above the Distributor (SASOL Wax, 20 wt% 0 – 5 μm Iron Oxide)

u_g	Radial Position[a]					
(m/s)	6.6	4.8	3.0	3.0	4.8	6.6
0.02	-0.016	0.055	0.005	0.037	0.035	0.047
0.04	0.337	0.382	0.289	0.314	0.172	0.071
0.06	0.238	0.300	0.297	0.226	0.210	0.081
0.09	0.203		0.313	0.189		-0.001
0.12	0.351	0.389	0.277	0.282	0.091	0.025
d_L^b	16.57	19.20	20.70	20.59	18.99	16.76
d_H^c	16.48	19.17	20.42	20.47	18.97	16.86

[a] – Measured from the center of the column (cm)
[b] – Distance through the column for the Cs–137 source (cm)
[c] – Distance through the column for the Co–60 source (cm)

Table 3.14b Gas and Solids Holdups from Measurements with the Nuclear Density Gauge at a Height of 1.5 m Above the Distributor After Modifying the Thickness (d) of the Absorbing Media (SASOL Wax, 20 wt% 0 – 5 μm Iron Oxide)

u_g	RADIAL POSITION[a]						ϵ_g^b	ϵ_g^c	ϵ_s^b	ϵ_s^c
(m/s)	6.6	4.8	3.0	3.0	4.8	6.6				
0.02	0.105	0.134	0.125	0.123	0.129	0.108	0.121	0.107	0.029	0.029
0.04	0.152	0.175	0.180	0.189	0.165	0.147	0.169	0.157	0.029	0.028
0.06	0.140	0.170	0.188	0.193	0.169	0.145	0.171	0.175	0.027	0.027
0.09	0.159		0.226	0.223		0.164	0.200	0.211	0.026	0.026
0.12	0.186	0.219	0.238	0.245	0.216	0.188	0.219	0.208	0.025	0.025
d_L^d	15.9-16.2	18.6-19.0	20.0-20.3	20.3-20.7	18.5-19.0	16.5-16.8				
d_H^e	16.48	19.17	20.42	20.47	18.97	16.86				

[a] – Measured from the center of the column (cm)
[b] – Axial holdups from nuclear density gauge measurements
[c] – Axial holdups from conventional measurements (Chapter II)
[d] – Range of values for the distance through the column for the Cs–137 source (cm)
[e] – Range of values for the distance through the column for the Co–60 source (cm)

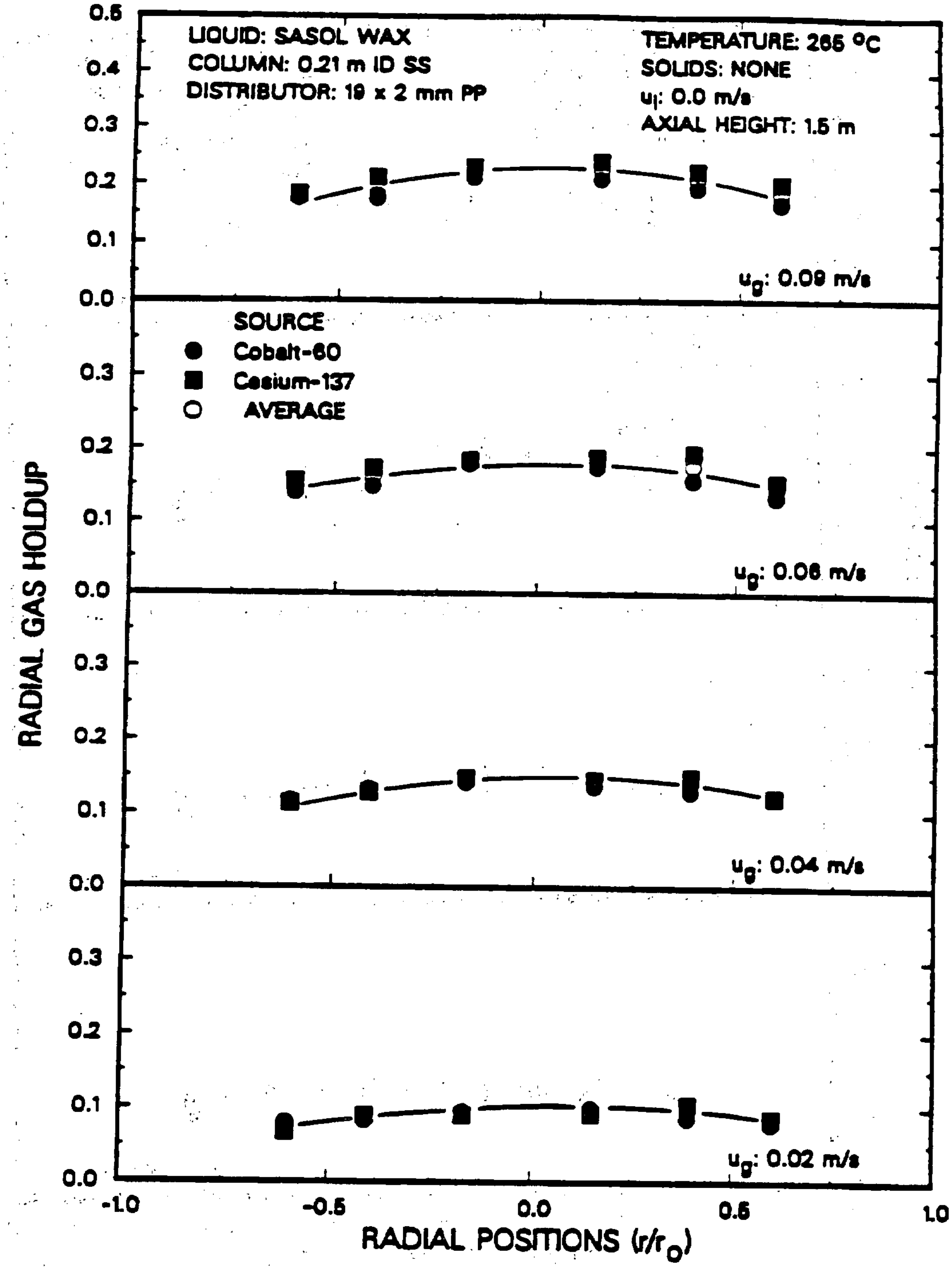

Figure 3.16. Effect of superficial gas velocity on radial gas holdup (SASOL wax, no solids, u_l = 0.0 m/s).

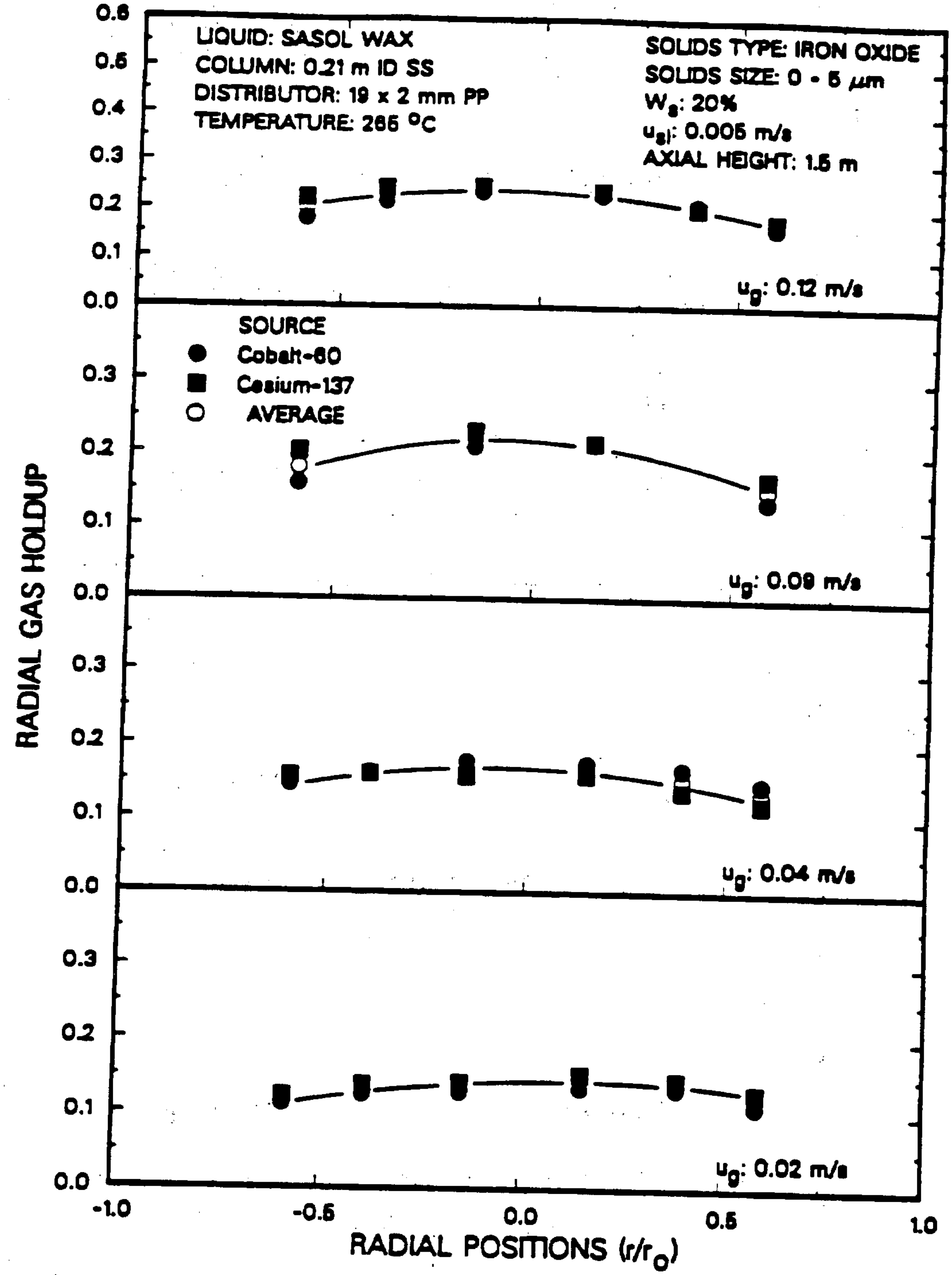

Figure 3.17. Effect of superficial gas velocity on radial gas holdup (SASOL wax, 20 wt% 0 - 5 μm iron oxide, u_{sl} = 0.005 m/s).

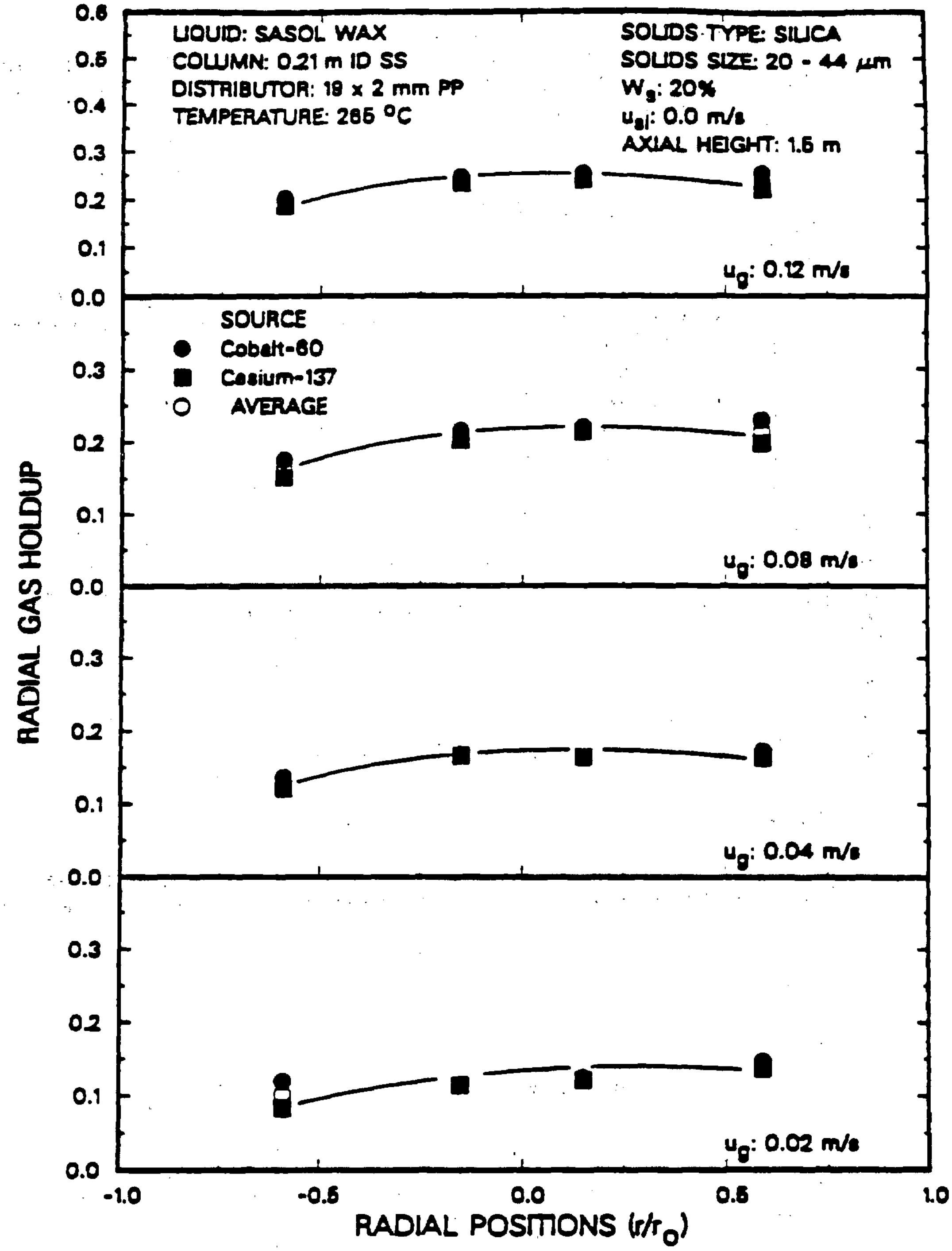

Figure 3.18. Effect of superficial gas velocity on radial gas holdup (SASOL wax, 20 wt% 20 - 44 μm silica, u_{sl} = 0.0 m/s).

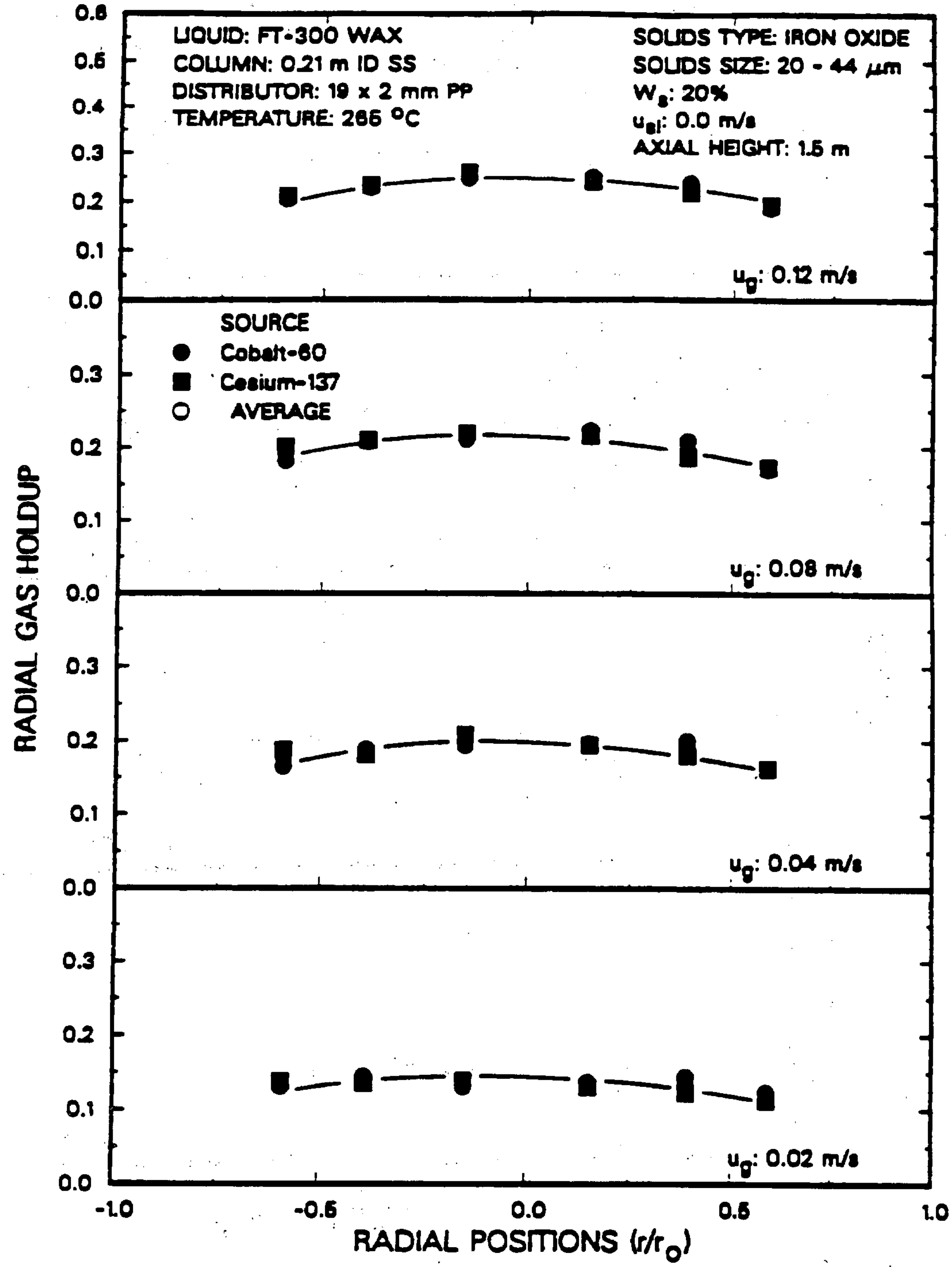

Figure 3.19. Effect of superficial gas velocity on radial gas holdup (FT-300 wax, 20 wt% 20 - 44 μm iron oxide, u_{sl} = 0.0 m/s).

were obtained using Eq. 3.37, and replacing the attenuation coefficient of the liquid, μ by the attenuation coefficient of the liquid/solid mixture – see Eq. 3.6). Since a pseudo two–phase system was assumed (three–phase systems), independent results could be obtained from each density gauge. For each case, independent results from the two density gauges are presented along with with average values of the radial gas holdup. The average values are simply an arithmetic average of the holdup values obtained from the two sources. In general, radial gas holdup profiles were fairly uniform at a gas velocity of 0.02 m/s, which was expected since flow is in the homogeneous bubbling regime at this velocity. However, as the gas velocity increases, the flow becomes slightly non–uniform with higher holdups in the center of the column. At higher gas velocities, larger gas bubbles are produced which tend to move upward through the center of the column and this in turn results in higher gas holdups in the center of the column. The trends observed at the other two heights (0.9 and 2.1 m) were similar to those shown at a height of 1.5 m above the distributor.

The radial holdups shown in Figures 3.16 to 3.19 are also presented in tabular form (see Tables 3.15 to 3.18, respectively). Also shown in these tables are the values of the attenuation coefficients and the initial (or empty column) count rates that were used. Empty column count rates at a given radial position did not vary by more than 2% between experiments. The empty column count rate decreases with increasing distance from the center of the column. This decrease in the count rate with increasing distance from the center of the column is because the thickness of the column changes due to its curvature (see Figure 3.20).

For all of the results shown in Figures 3.17 to 3.19 (three–phase systems), the attenuation coefficient was assumed to be constant at all gas velocities, since the solids concentration did not vary significantly with gas velocity in the large column (see Chapter IV), with the exception of the experiments conducted with large iron oxide particles.

Table 3.15a. Radial Gas Holdups Obtained Using the Co–60 Source (SASOL Wax, No Solids, u_ℓ = 0 m/s)

u_g (m/s)	$\mu_{s\ell}$ (cm^{-1})	Radial Position[a] 6.6	4.8	3.0	3.0	4.8	6.6
0.02	0.0415	0.102	0.113	0.145	0.115	0.111	0.101
0.04	0.0415	0.132	0.143	0.154	0.146	0.135	0.136
0.06	0.0415	0.151	0.178	0.178	0.183	0.180	0.156
0.09	0.0415	0.171	0.209	0.219	0.223	0.212	0.181
B_o^b		3582	3805	3926	3957	3852	3742
d^c		16.10	17.70	19.18	19.43	18.16	16.40

[a] – Measured from the center of the column (cm)
[b] – Empty column count rate (counts/sec)
[c] – Distance through the column (cm)

Table 3.15b. Radial Gas Holdups Obtained Using the Cs–137 Source (SASOL Wax, No Solids, u_ℓ = 0 m/s)

u_g (m/s)	$\mu_{s\ell}$ (cm^{-1})	Radial Position[a] 6.6	4.8	3.0	3.0	4.8	6.6
0.02	0.0519	0.106	0.109	0.117	0.118	0.095	0.099
0.04	0.0519	0.141	0.155	0.167	0.158	0.137	0.136
0.06	0.0519	0.171	0.190	0.199	0.204	0.170	0.175
0.09	0.0519	0.205	0.229	0.245	0.246	0.212	0.202
B_o^b		1958	2082	2149	2164	2120	2011
d^c		16.20	18.78	20.60	20.70	19.23	17.38

[a] – Measured from the center of the column (cm)
[b] – Empty column count rate (counts/sec)
[c] – Distance through the column (cm)

Table 3.16a. Radial Gas Holdups Obtained Using the Co-60 Source (SASOL Wax, 20 wt% 0 - 5 μm Iron Oxide, u_{sl} = 0.005 m/s)

u_g (m/s)	μ_{sl} (cm^{-1})	Radial Position[a] 6.6	4.8	3.0	3.0	4.8	6.6
0.02	0.0494	0.111	0.134	0.135	0.128	0.126	0.113
0.04	0.0494	0.147	0.149	0.174	0.176	0.161	0.145
0.06	0.0494	0.149	0.177	0.192	0.191	0.173	0.157
0.09	0.0494	0.171		0.214	0.209		0.177
0.12	0.0494	0.199	0.209	0.231	0.235	0.215	0.197
B_o^b		3618	3828	3903	3901	3815	3677
d^c		16.48	19.17	20.42	20.47	18.97	16.86

a - Measured from the center of the column (cm)
b - Empty column count rate (counts/sec)
c - Distance through the column (cm)

Table 3.16b. Radial Gas Holdups Obtained Using the Cs-137 Source (SASOL Wax, 20 wt% 0 - 5 μm Iron Oxide, u_{sl} = 0.005 m/s)

u_g (m/s)	μ_{sl} (cm^{-1})	Radial Position[a] 6.6	4.8	3.0	3.0	4.8	6.6
0.02	0.0635	0.129	0.146	0.154	0.142	0.138	0.122
0.04	0.0635	0.121	0.137	0.181	0.157	0.160	0.145
0.06	0.0635	0.157	0.159	0.176	0.187	0.168	0.158
0.09	0.0635	0.167		0.215	0.230		0.192
0.12	0.0635	0.210	0.203	0.239	0.246	0.242	0.211
B_o^b		2007	2116	2174	2185	2108	1997
d^c		16.57	19.20	20.70	20.59	18.99	16.76

a - Measured from the center of the column (cm)
b - Empty column count rate (counts/sec)
c - Distance through the column (cm)

Table 3.17a. Radial Gas Holdups Obtained Using the Co-60 Source
(SASOL Wax, 20 wt% 20 – 44 μm Silica, $u_{s\ell}$ = 0 m/s)

u_g (m/s)	$\mu_{s\ell}$ (cm^{-1})	Radial Position[a] 6.6	3.0	3.0	6.6
0.02	0.0478	0.131	0.125	0.115	0.111
0.04	0.0478	0.157	0.164	0.167	0.128
0.08	0.0478	0.214	0.219	0.214	0.167
0.12	0.0478	0.235	0.254	0.246	0.196
B_o[b]		3619	3953	3970	3675
d[c]		16.55	20.31	20.41	15.9

[a] – Measured from the center of the column (cm)
[b] – Empty column count rate (counts/sec)
[c] – Distance through the column (cm)

Table 3.17b. Radial Gas Holdups Obtained Using the Cs-137 Source
(SASOL Wax, 20 wt% 20 – 44 μm Silica, $u_{s\ell}$ = 0 m/s)

u_g (m/s)	$\mu_{s\ell}$ (cm^{-1})	Radial Position[a] 6.6	3.0	3.0	6.6
0.02	0.0642	0.137	0.121	0.114	0.084
0.04	0.0642	0.163	0.164	0.166	0.121
0.06	0.0642	0.198	0.213	0.201	0.151
0.12	0.0642	0.219	0.239	0.232	0.186
B_o[b]		2049	2226	2230	2050
d[c]		16.65	20.44	20.49	16.0

[a] – Measured from the center of the column (cm)
[b] – Empty column count rate (counts/sec)
[c] – Distance through the column (cm)

Table 3.18a. Radial Gas Holdups Obtained Using the Co–60 Source
(FT–300 Wax, 20 wt% 20 – 44 μm Iron Oxide, u_{sl} = 0 m/s)

u_g (m/s)	μ_{sl} (cm^{-1})	Radial Position[a] 6.6	4.8	3.0	3.0	4.8	6.6
0.02	0.0466	0.123	0.144	0.137	0.131	0.144	0.131
0.04	0.0495	0.163	0.199	0.197	0.193	0.188	0.165
0.08	0.0495	0.170	0.208	0.223	0.211	0.208	0.183
0.12	0.0495	0.188	0.238	0.250	0.248	0.228	0.204
B_o^b		3603	3821	3941	3981	3837	3691
d^c		16.49	18.76	20.06	20.07	18.77	15.81

[a] – Measured from the center of the column (cm)
[b] – Empty column count rate (counts/sec)
[c] – Distance through the column (cm)

Table 3.18b. Radial Gas Holdups Obtained Using the Cs–137 Source
(FT–300 Wax, 20 wt% 20 – 44 μm Iron Oxide, u_{sl} = 0 m/s)

u_g (m/s)	μ_{sl} (cm^{-1})	Radial Position[a] 6.6	4.8	3.0	3.0	4.8	6.6
0.02	0.0619	0.112	0.122	0.130	0.139	0.136	0.138
0.04	0.0662	0.163	0.181	0.194	0.208	0.181	0.187
0.08	0.0662	0.173	0.189	0.216	0.219	0.210	0.200
0.12	0.0662	0.194	0.228	0.242	0.259	0.236	0.210
B_o^b		2065	2197	2252	2273	2216	2102
d^c		16.96	18.17	20.26	19.85	18.83	15.79

[a] – Measured from the center of the column (cm)
[b] – Empty column count rate (counts/sec)
[c] – Distance through the column (cm)

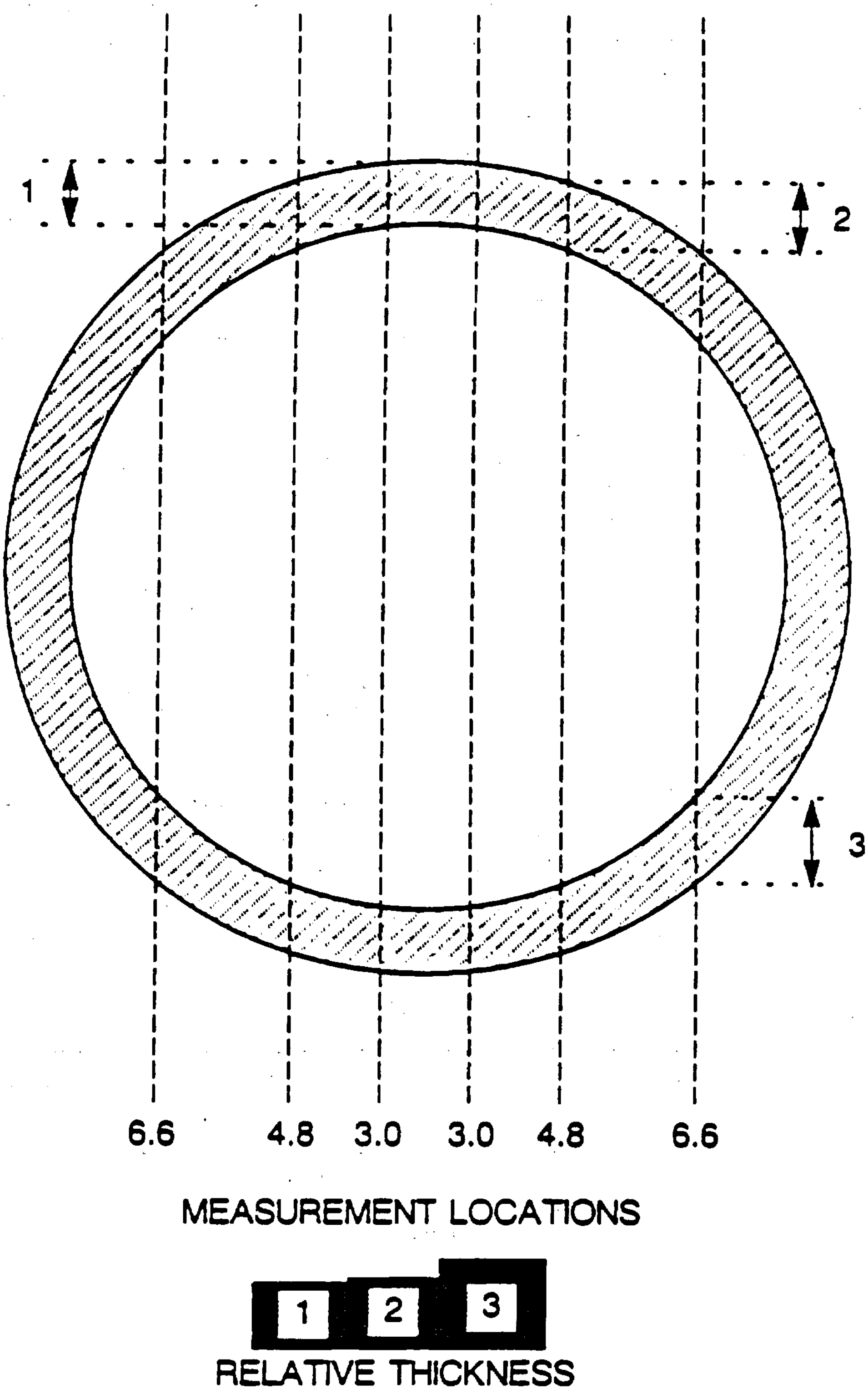

Figure 3.20. Schematic representation of bubble column wall.

During these experiments, the solids concentration in the column was lower at a velocity of 0.02 m/s than at higher gas velocities and thus, the attenuation coefficient of the slurry at this gas velocity was different than those at other velocities (see Table 3.18).

Figures 3.21a and 3.21b compare average gas holdup values obtained using pressure measurements to those obtained with the nuclear density gauges for experiments with SASOL wax (no solids) at liquid velocities of 0 m/s and 0.005 m/s, respectively. There is very good agreement between different sets of values for both runs. For the batch experiment (Figure 3.20a), gas holdup values obtained using pressure measurements were somewhat lower than those from the density gauge using the Cs–137 source and comparable to those obtained with the density gauge using the Co–60 source.

Figures 3.22a, 3.22b, and 3.22c compare average gas holdups from pressure measurements with those obtained using the nuclear density gauges for experiments with SASOL wax (20 wt% 0 – 5 μm iron oxide particles) at slurry velocities of 0 m/s, 0.[illegible] m/s, and 0.02 m/s, respectively. There is excellent agreement in results obtained in the continuous mode of operation (Figures 3.22a and 3.22b) using the different methods. However, for the batch experiment, gas holdup values obtained using pressure measurements were consistently lower than those obtained using either of the density gauges. As mentioned previously, average gas holdups for the NDG technique were calculated by simply using an arithmetic average of the axial gas holdups (see Eq. 3.45). In order to determine if this method for calculating the average gas holdups caused the differences, average holdups were also calculated by fitting the data to a curve and integrating across the expanded height (see Eq. 3.44). While average holdups were slightly lower using this technique (between 0.4% and 2.0% - relative), they were still higher than the values obtained using the pressure transducers. Axial gas holdups measured using the density gauges for this experiment at gas velocities of 0.04 and 0.09 m/s are compared

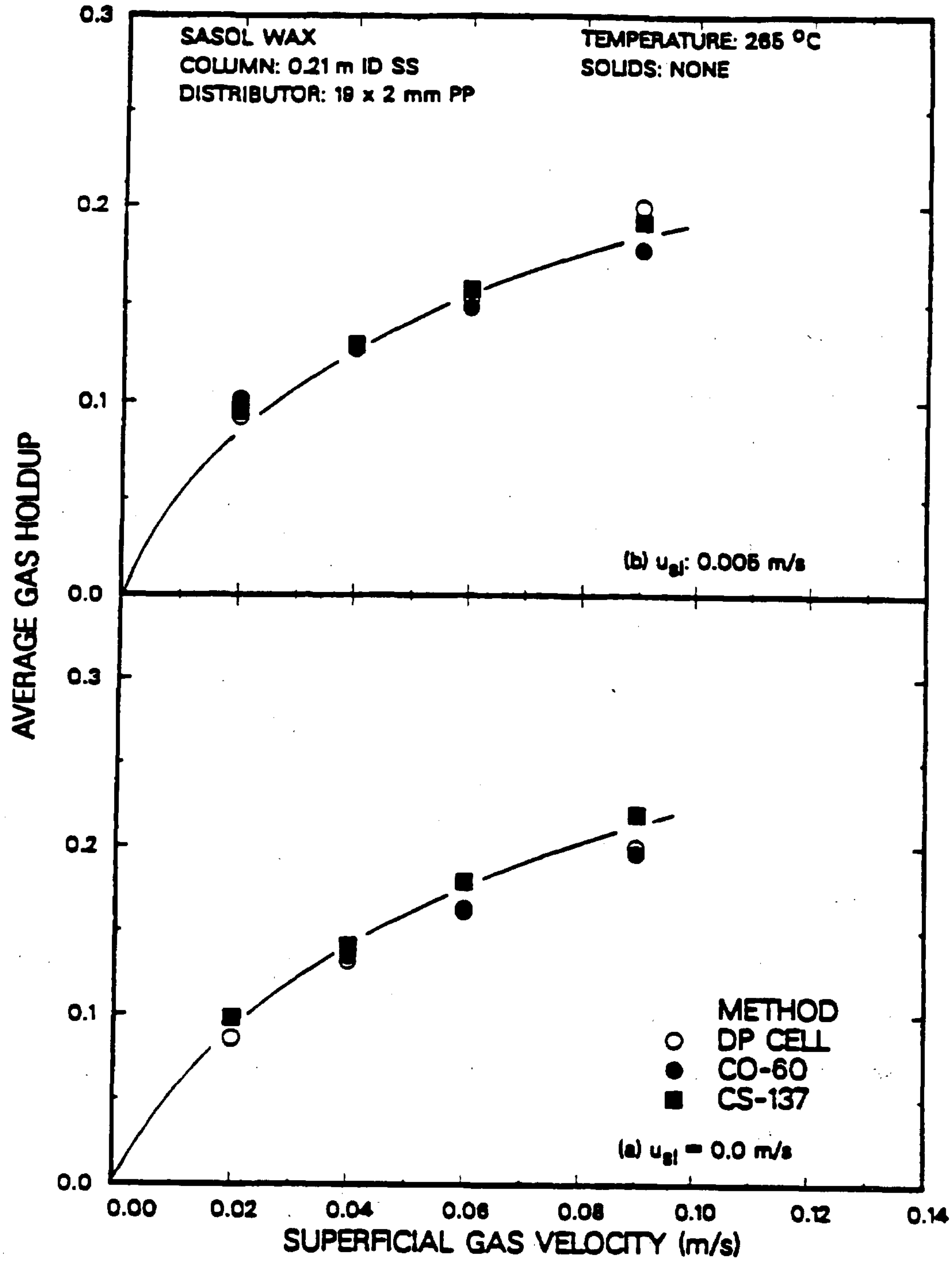

Figure 3.21. Comparison of average gas holdups from the DP cells and nuclear density gauges (SASOL wax, no solids; (a) u_l = 0.0 m/s; (b) u_l = 0.005 m/s).

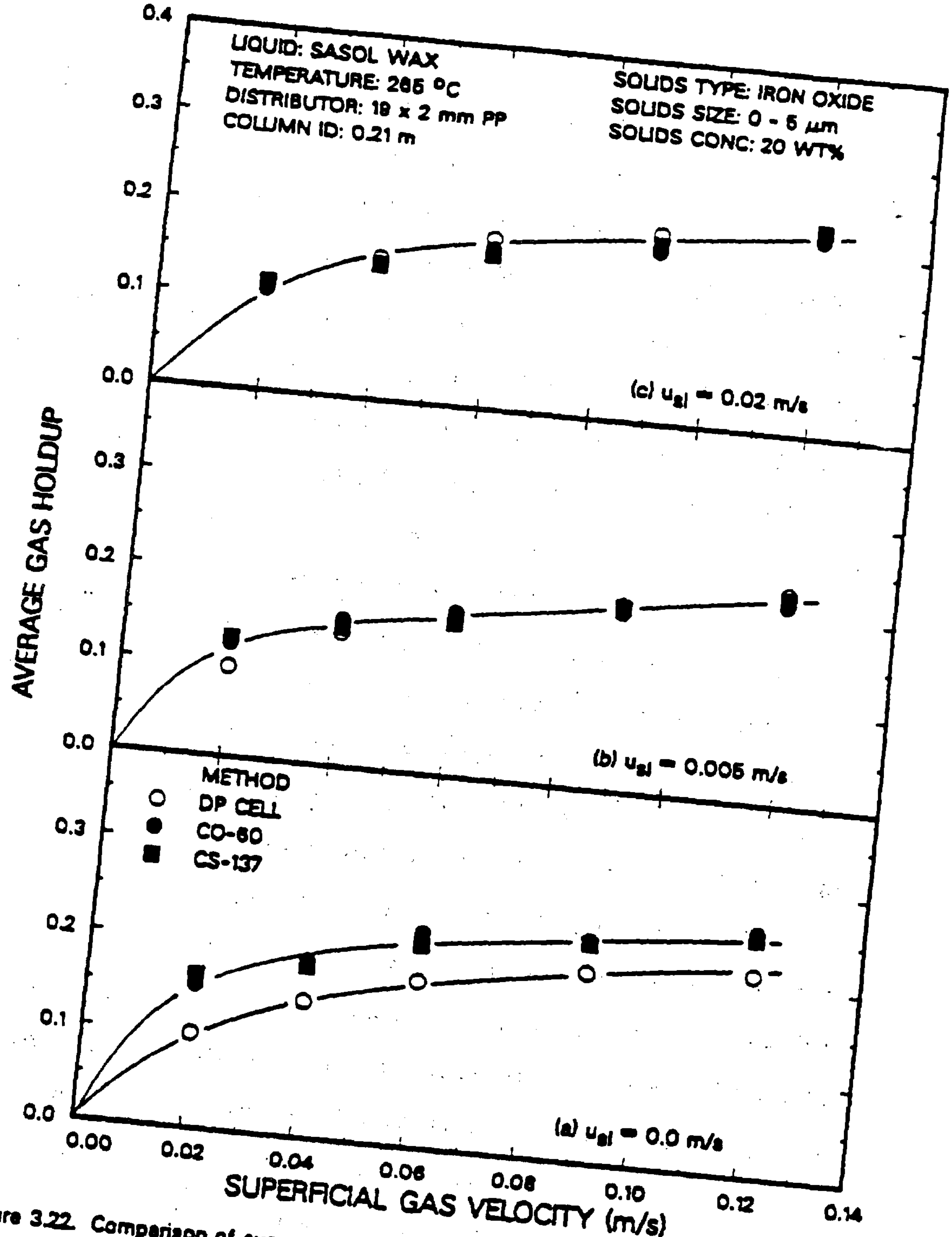

Figure 3.22. Comparison of average gas holdups from the DP cells and nuclear density gauges (SASOL wax, 20 wt% 0 - 5 μm iron oxide; (a) u_{sl} = 0.0 m/s, (b) u_{sl} = 0.005 m/s, (c) u_{sl} = 0.02 m/s).

to axial gas holdups obtained using pressure measurements in Figure 3.23a and 3.23b, respectively. At a gas velocity of 0.04 m/s, the axial gas holdups obtained from pressure measurements were somewhat lower than those obtained using the density gauge. At the present time, we do not know what caused this difference (i.e. if it was due to errors in pressure readings, solids concentrations, or density gauge measurements). At a gas velocity of 0.09 m/s, axial gas holdups obtained from pressure measurements and density gauge measurements were comparable. However, in the bottom most section of the column (0.31 m), the axial gas holdup (pressure measurements) is considerably lower. As a result, the average gas holdup obtained from the density gauges is higher than that obtained from the pressure measurements. This implies, that if axial gas holdups vary considerably over the height of the dispersion, more measurements with the density gauge are needed to obtain an accurate estimate for the average gas holdup. As shown in Figure 2.15, axial gas holdups from continuous experiments varied almost linearly with height. Thus, it is not surprising that average gas holdups obtained with the density gauge were comparable to those obtained with the pressure transducers.

Average gas holdup results from batch experiments with 20 wt% large iron oxide and silica particles are shown in Figures 3.24a and 3.24b, respectively. Once again, gas holdups from the two density gauges were comparable. However, gas holdup values obtained by conventional techniques (pressure measurements) were lower, especially for the experiment with large iron oxide particles. During this experiment, axial gas holdups in the bottom section of the column (i.e. 0.31 m above the distributor) were substantially lower than those at heights of 0.9, 1.5 and 2.1 m as shown in Figure 3.25a and 3.25b. Axial gas holdups from pressure measurements and density gauge measurements were comparable at heights of 0.9, 1.5, and 2.1 m above the distributor, once again indicating that a better estimate for the average gas holdup would be obtained if measurements were made at additional axial positions. During the experiment with large

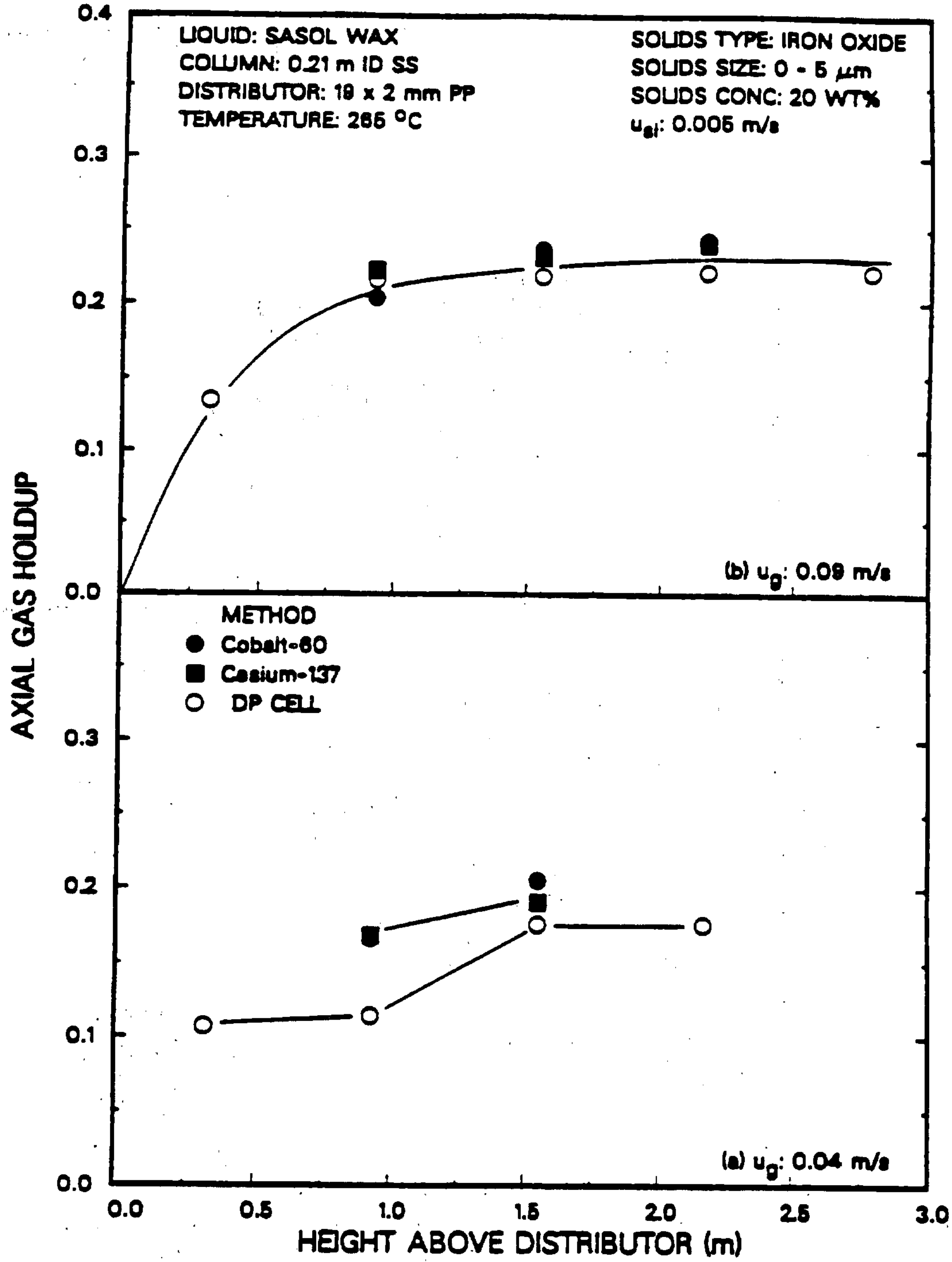

Figure 3.23. Comparison of axial gas holdups from the DP cells and nuclear density gauges (SASOL wax, no solids; (a) u_g = 0.04 m/s; (b) u_g = 0.09 m/s).

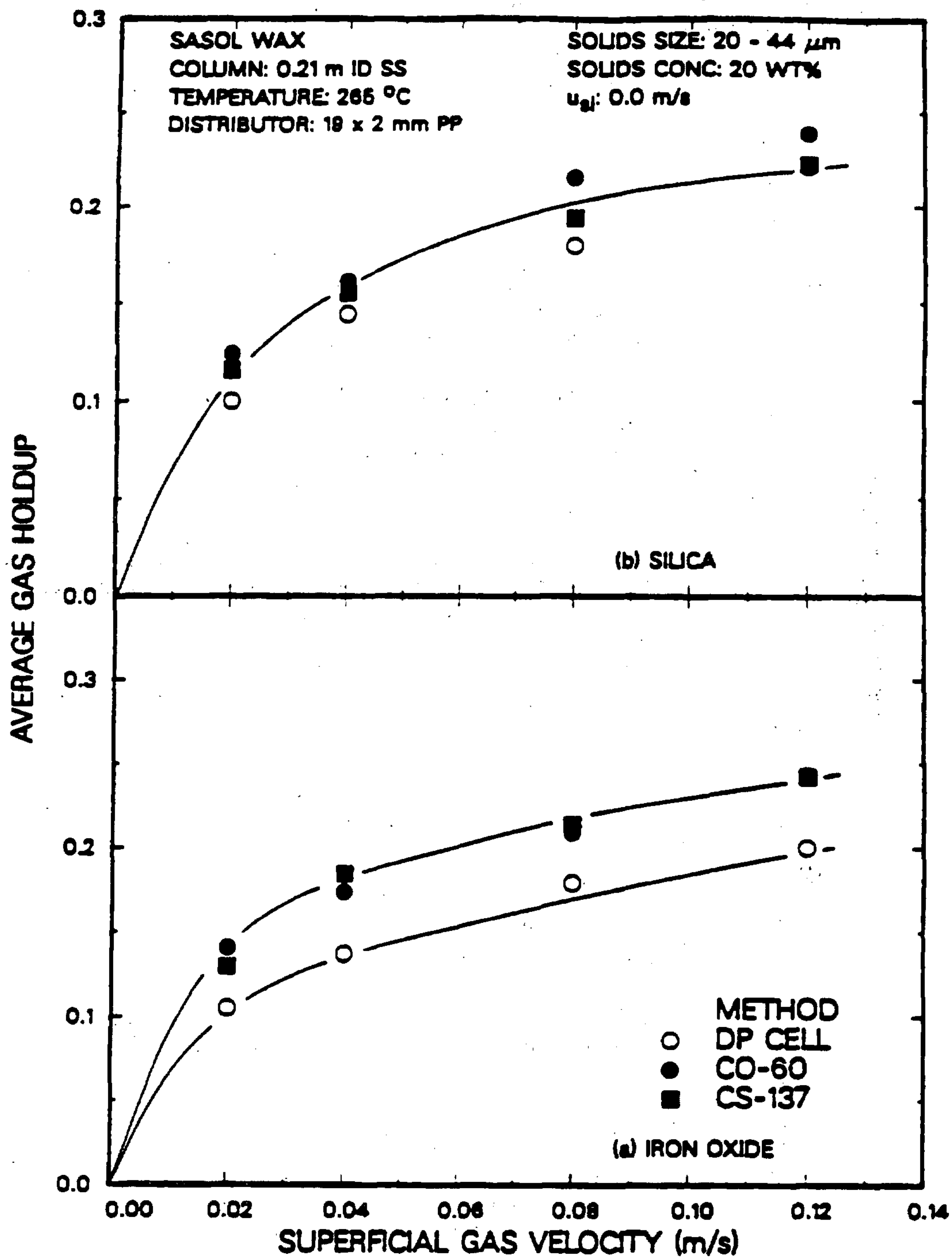

Figure 3.24. Comparison of average gas holdups from the DP cells and nuclear density gauges (SASOL wax; u_{sl} = 0.0 m/s; (a) 20 wt% 20 - 44 μm iron oxide; (b) 20 wt% 20 - 44 μm silica).

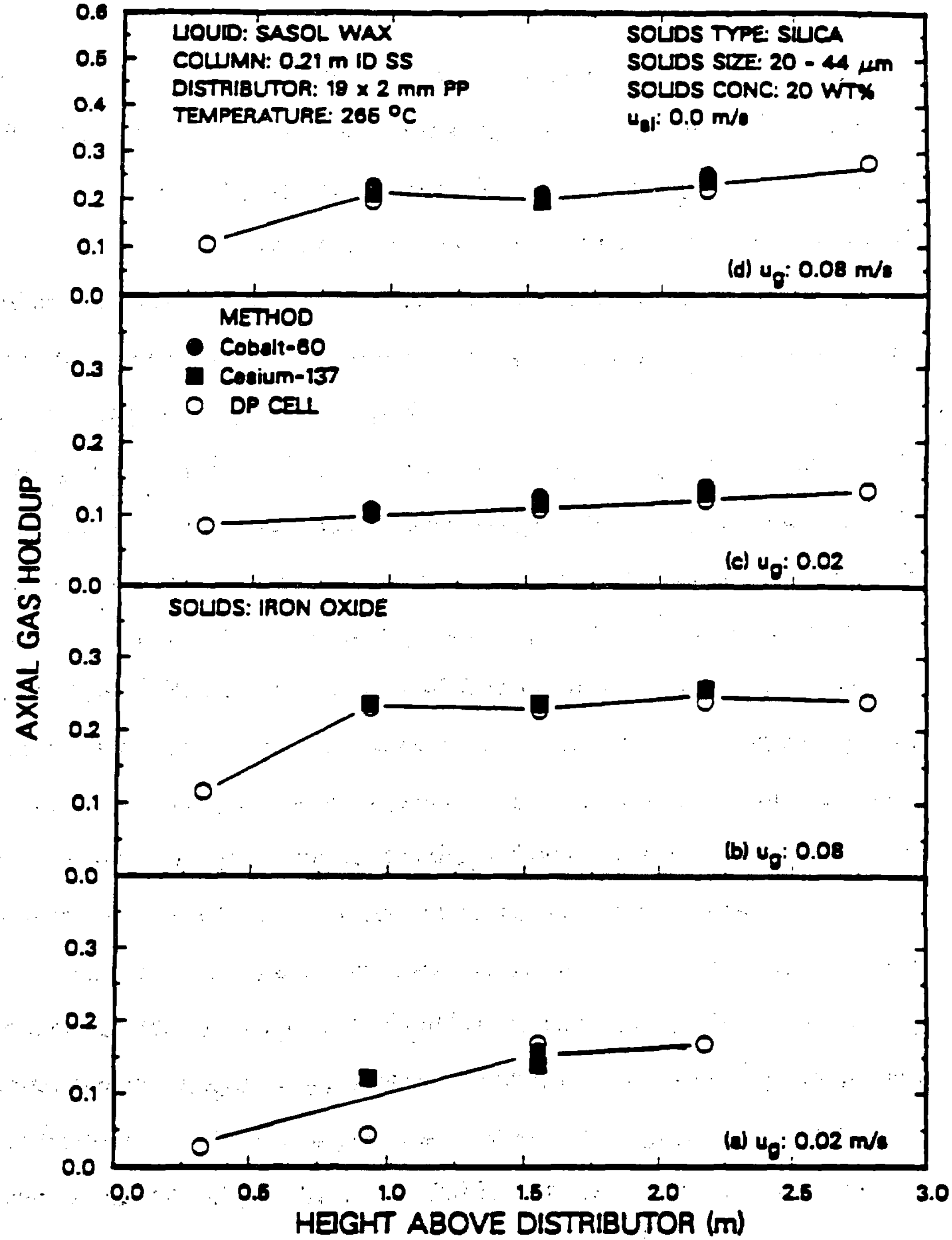

Figure 3.25. Comparison of axial gas holdups from the DP cells and nuclear density gauges (SASOL wax, 20 wt% 20 - 44 μm iron oxide - (a) u_g = 0.02 m/s; (b) u_g = 0.08 m/s; SASOL wax, 20 wt% 20 - 44 μm silica - (c) u_g = 0.02 m/s; (d) u_g = 0.08 m/s).

silica particles, we did not observe as significant difference in axial gas holdups between heights of 0.3 and 0.9 m above the distributor (see Figure 3.25c and 3.25d), consequently, the average gas holdup values obtained using the density gauges compared favorable with those obtained using the pressure transducers.

Figure 3.26 compares average gas holdup values from pressure measurements with those obtained from density gauge measurements for experiments with FT–300 wax. In particular, Figures 3.26a and 3.26b show results from two–phase experiments at slurry velocities of 0.0 and 0.005 m/s, respectively. There is excellent agreement in gas holdups obtained using both pressure measurements and density gauge measurements. For the batch mode experiment with large iron oxide particles, average gas holdups from pressure measurements and density gauge measurements were comparable at all gas velocities except at a velocity of 0.04 m/s (see Figure 3.26c). At this gas velocity, the average gas holdup obtained from pressure measurements was substantially larger than that obtained from density gauge measurements. Once again, this difference is due to the fact that measurements with the density gauges were made at only three positions (i.e. 0.9, 1.5, and 2.1 m); whereas, measurements with the pressure transducers were made at five positions. For this experiment, foam the uppermost region of the column (i.e. above 2.1 m), and the axial gas holdup in this region was 0.68. Since density gauge measurements were limited to heights below this, the average gas holdup estimated from analysis of density gauge data (for both sources) was less than the actual gas holdup.

Axial gas holdups at velocities of 0.04 and 0.12 m/s for the two experiments with no solids are presented in Figure 3.27. The axial gas holdup profile obtained from pressure measurements did not vary significantly with axial position during either of these experiments. Axial gas holdups obtained from density gauge measurements were similar to those obtained from pressure measurements. Axial gas holdups did not vary significantly over the length of the column, and since axial gas holdups from conventional

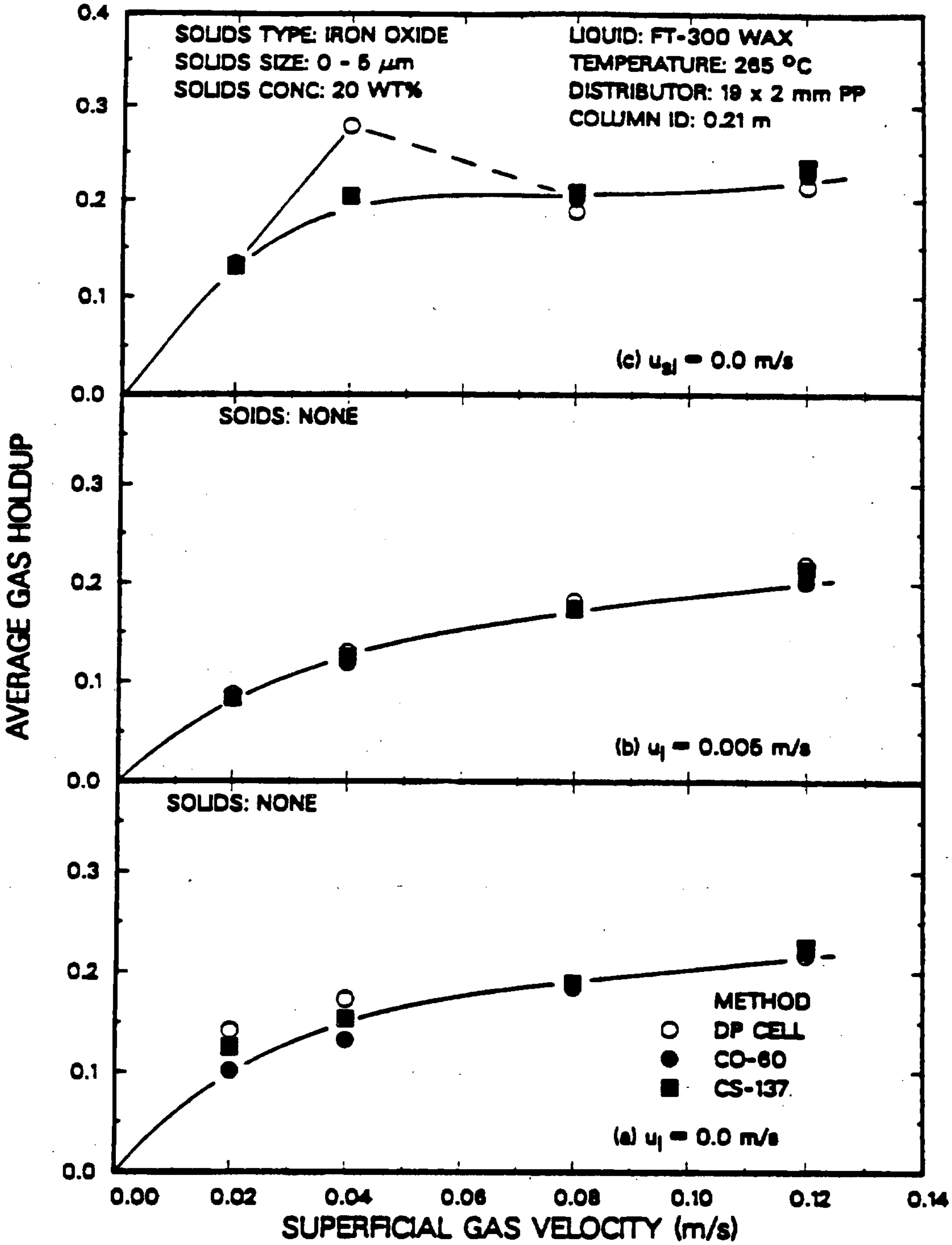

Figure 3.26. Comparison of average gas holdups from the DP cells and nuclear density gauges (FT-300 wax; (a) u_l = 0.0 m/s, no solids; (b) u_l = 0.005 m/s, no solids; (c) u_{sl} = 0.0 m/s, 20 wt% 20 - 44 μm iron oxide).

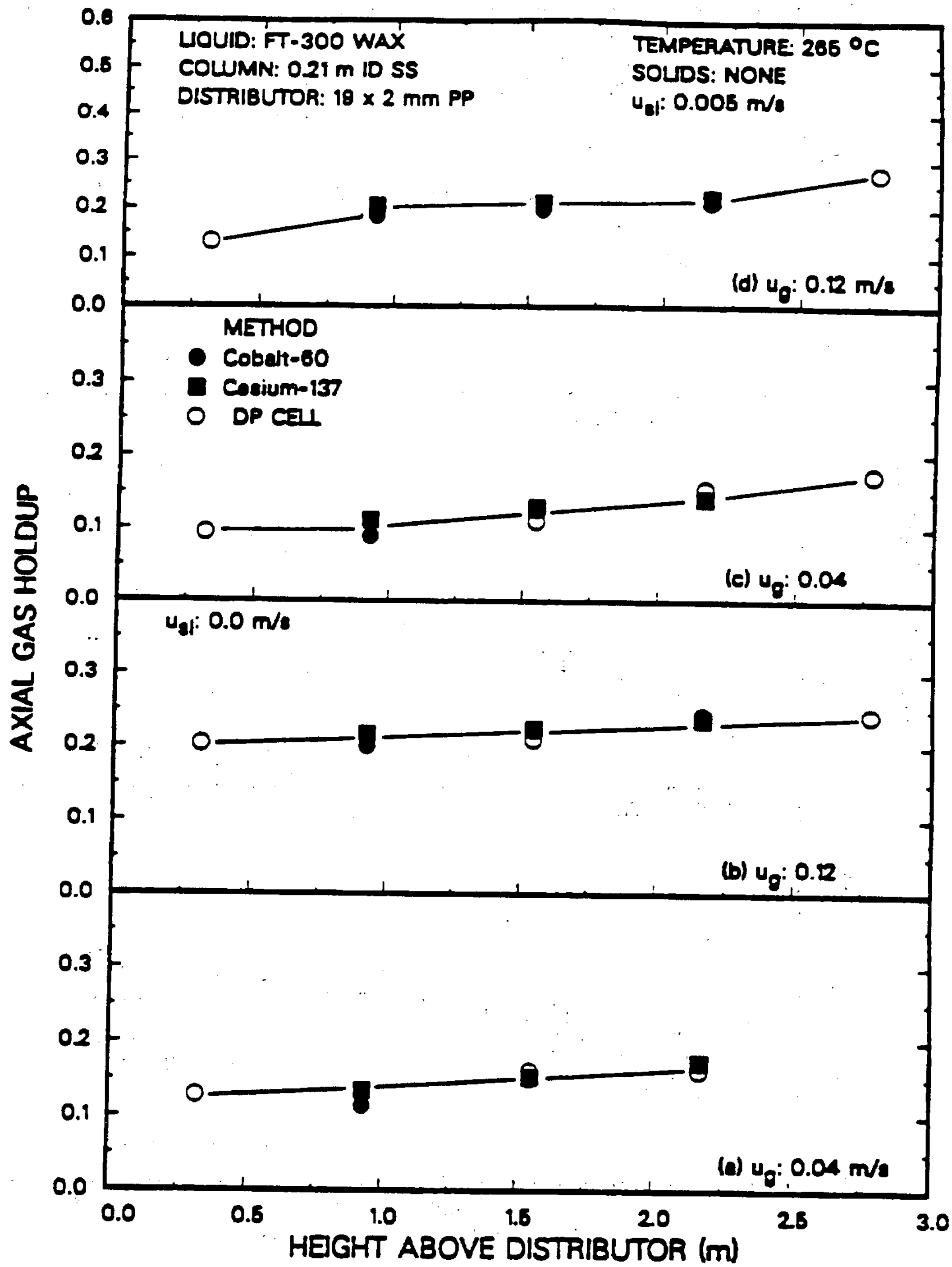

Figure 3.27. Comparison of axial gas holdups from the DP cells and nuclear density gauges with FT-300 wax and no solids (u_l = 0.0 m/s - (a) u_g = 0.04 m/s; (b) u_g = 0.12 m/s; u_l = 0.005 m/s - (c) u_g = 0.04 m/s; (d) u_g = 0.12 m/s).

measurements and density gauge measurements were comparable at heights of 0.9, 1 and 2.1 m above the distributor, it is not surprising that there was excellent agreement in average gas holdups obtained from the different techniques. Figure 3.28 shows axial gas holdups obtained from the batch experiment with large iron oxide particles (see Figure 3.26c) at gas velocities of 0.02, 0.04, and 0.08 m/s. During this experiment axial gas holdups almost varied linearly with height above the distributor, with the exception of the axial gas holdup in the uppermost section of the column at a gas velocity of 0.04 m/s. Thus, average gas holdups obtained from the pressure measurements are higher than those obtained from the density gauge measurements at this gas velocity.

Overall, axial gas holdups obtained from the nuclear density gauges compared favorably with those obtained using pressure measurements. For experiments in which either there was not a significant gradient in axial gas holdups, or where axial gas holdup increased linearly with height the average gas holdup values from the different methods were similar. Based on our results from pressure measurements, it appears that ax gas holdups are essentially uniform (or vary only slightly) in the central portion of the column; however, in the uppermost region of the column, or at the bottom of the column, axial gas holdups can be substantially different. Thus, a better estimate of the average gas holdup could be obtained if density gauge measurements were made in the top and bottom regions of the column.

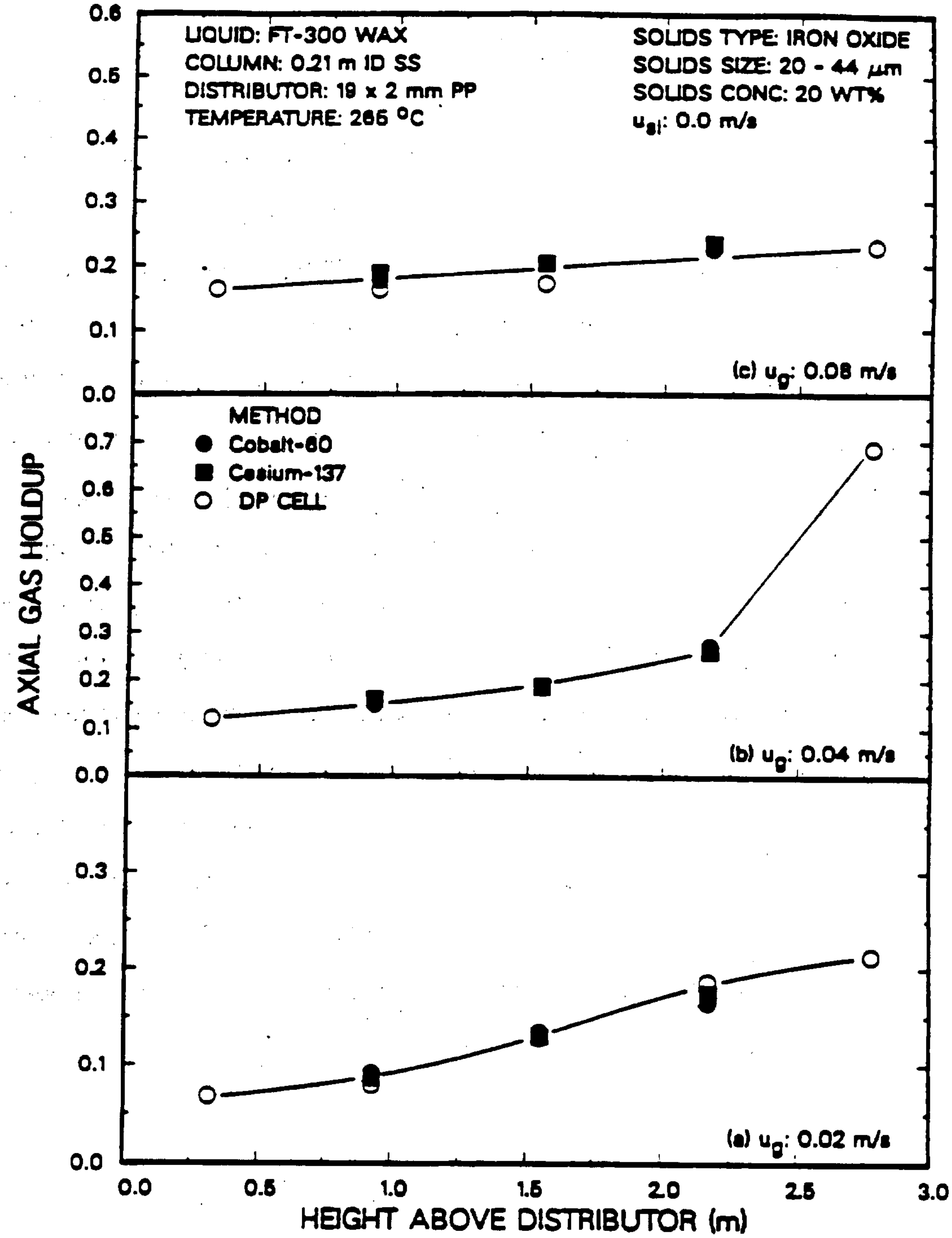

Figure 3.28. Comparison of axial gas holdups from the DP cells and nuclear density gauges (FT-300 wax, 20 wt% 20 - 44 μm iron oxide - (a) $u_g = 0.02$ m/s; (b) $u_g = 0.04$ m/s; (c) $u_g = 0.08$ m/s).